

Electroluminescence of an n-ZnO/p-GaN Heterojunction under Forward and Reverse Biases *

QIN Qi(秦琦), GUO Li-Wei(郭丽伟), ZHOU Zhong-Tang(周忠堂), CHEN Hong(陈弘),
DU Xiao-Long(杜小龙), MEI Zeng-Xia(梅增霞), JIA Jin-Feng(贾金峰), XUE Qi-Kun(薛其坤),
ZHOU Jun-Ming(周均铭)**

State Key Laboratory for Surface Physics, Institute of Physics, Chinese Academy of Sciences, Beijing 100080

(Received 10 May 2005)

Electroluminescent characteristics of n-ZnO/p-GaN heterojunctions under forward and reverse biases are studied. Emissions at 389 nm and 570 nm are observed under forward bias. An unusual emission at 390 nm appears under reverse bias, and is attributed to the recombination in the p-GaN side of the heterojunction. The yellow emission peaked at 570 nm is suppressed under reverse bias. The light intensity exponentially depends on the reverse current. The emission under reverse bias is correlated to tunnelling carrier transport in the heterostructure. Our results also support that the well-known yellow band of GaN comes from the transitions between some near-conduction-band-edge states and deep localized acceptor states.

PACS: 42.72.Bj, 78.30.Fs, 78.55.-m, 78.60.Fi

Wide bandgap (3.37 eV at room temperature) ZnO is a promising material for the application of short wavelength exciton-based optoelectronic devices^[1-3] due to its larger exciton binding energy of 60 meV.^[4] Amenability to conventional chemical wet etching and availability of large area substrates at relatively low cost^[5] further increase its application potential. However, difficult p-type doping in ZnO impedes the fabrication of ZnO-based light-emitting diodes (LEDs) and laser diodes (LDs) despite some progress in p-type crystal growth.^[6-9] ZnO and GaN are similar in many aspects of their physical properties, such as the same wurtzite crystal structure, similar in-plane lattice parameter and energy bandgap. N-ZnO/p-GaN heterojunction has been recently suggested^[10,11] and fabricated^[12-15] to overcome the problem in p-doping. In those works, EL and PL of the n-ZnO/p-GaN heterojunction were carefully studied. However, EL was observed under only one kind of bias, either forward (390 nm,^[12] 430 nm^[13] and 384 nm^[15]) or reverse (450 nm and 560 nm^[14]). In this Letter, we report the EL characteristics of an n-ZnO/p-GaN heterojunction under forward and reverse biases, respectively. Different from other reports, under forward bias there are two EL peaks (one is at 389 nm related to transition from the conduction band to a shallow Mg acceptor, and the other at 570 nm corresponding to the yellow band emission in p-GaN), only 390 nm peak was observed under the reverse bias, which is ascribed to a recombination process in the p-GaN side at the interface assisted by tunnelling carrier transport. Our results further demonstrate that the commonly observed yellow band is indeed related to the recombination of the

electrons near the conduction-band edge states with the holes in deep localized acceptor states.^[16-19]

Our n-ZnO samples were grown by rf-MBE on p-GaN substrate, which was previously prepared in a metal-organic chemical vapor deposition system. The details of Mg-doped GaN growth can be found elsewhere.^[20] The p-type GaN film has a thickness of about 2 μm , with a carrier concentration of about $1 \times 10^{17} \text{ cm}^{-3}$ and room temperature hole mobility of about $6 \text{ cm}^2 \text{ V}^{-1} \text{ s}^{-1}$. Before the ZnO deposition, the GaN film was first cleaned by *in situ* thermal annealing and nitrogen plasma irradiation at 700°C. Zn and Ga were supplied by evaporating 6N elemental Zn and 7N Ga from commercial Knudsen cells. An oxygen purifier (SAES) was used to purify the 5N O₂. Gas flow rate was controlled by mass flow controllers (ROD-4, Aera). An rf-plasma gun was used to produce active oxygen radicals. A Ga-doped ZnO layer was grown at 680°C for two hours with a growth rate of 6 nm/min. The Hall measurement showed that the electron concentration is $1.2 \times 10^{18} \text{ cm}^{-3}$, and the room temperature mobility is $45 \text{ cm}^2 \text{ V}^{-1} \text{ s}^{-1}$.

For convenience of device fabrication, a large size device ($\sim 55 \text{ mm}^2$) is processed. The large size results in high series resistance and thus high partial voltage in the applied voltage, which will be observed in the EL spectra. The surface of n-ZnO was etched by using 10% HNO₃ aqueous solution before the ohmic contact process. The ohmic contacts on the n-ZnO and p-GaN were realized by depositing Ti/Au and Ni/Au, respectively, followed by a rapid thermal annealing at 520°C.

For our samples, light emission was strong even

* Supported by the National Natural Science Foundation under Grant Nos 60476044, 60376004 and 60021403, and the National Key Basic Research and Development Programme of China under Grant Nos 2002CB311903 and 2002CB613500.

** To whom correspondence should be addressed. Email: jmzhou@aphy.iphy.ac.cn

by native eyes under both the forward and reverse bias. Figure 1 shows the EL spectra under the forward biases: two emission peaks are clearly observed. One is an ultraviolet emission band at 389 nm with an FWHM of about 40 nm, and the other is a broad luminescence band centred at 570 nm, the well-known yellow band. As the forward bias increases from 30 to 70 V in steps of 10 V, both the emissions show an increase of intensity without distinct peak shift. However, the intensity of the 389 nm peak exceeds the one at 570 nm when applied forward voltage is larger than 60 V due to the saturation of the yellow band state. The 389 nm peak comes from the transmission from the conduction band to a shallow Mg acceptor,^[21–26] which is further confirmed by the room-temperature photoluminescence (PL) experiment shown in the following.

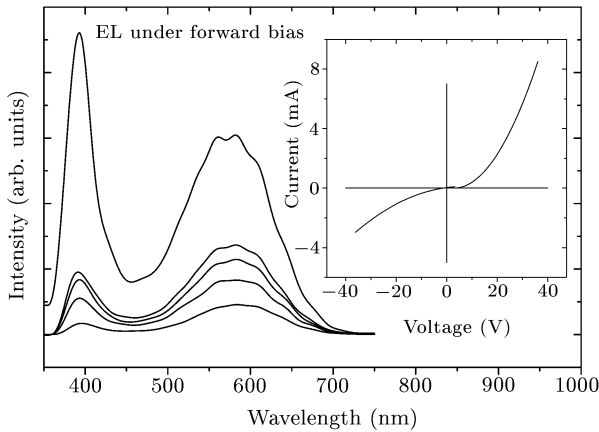


Fig. 1. EL spectra of the *n*-ZnO/*p*-GaN heterojunction under different forward voltages (from 30 V to 70 V in steps of 10 V, with the sequence from bottom to top). The inset shows the *I*-*V* characteristics.

As shown in the inset of Fig. 1, the *I*-*V* characteristic shows a rectifying diode feature. From the figure, it is shown that the turn-on voltage is about 6 V although it is soft due to the large series resistance of the device. Under the reverse bias, the breakdown is soft also due to the possible effect of defects^[13] and the breakdown voltage is about 7 V assigned as the voltage where the leakage current is about 10^{-4} A. Compared with the other result, our turn-on voltage is slightly higher because the doping concentration of our heterostructure diode is not high enough. The behaviour under the reverse bias is different from a standard *p*-*n* junction, which should show a sharp current increase at a large reverse voltage. In our case, the reverse current also increases softly with increasing reverse voltage. Figure 2 shows the EL spectrum under different reverse voltage, which shows only one dominant emission centred at 390 nm and is different from the spectra under forward bias (Fig. 1). Meanwhile, the emission peak is broadened by a long tail in the long

wavelength (to 650 nm). The EL emission exhibits the similar bias dependence of its intensity and peak position (from 30 to 90 V), compared to the case under the forward bias.

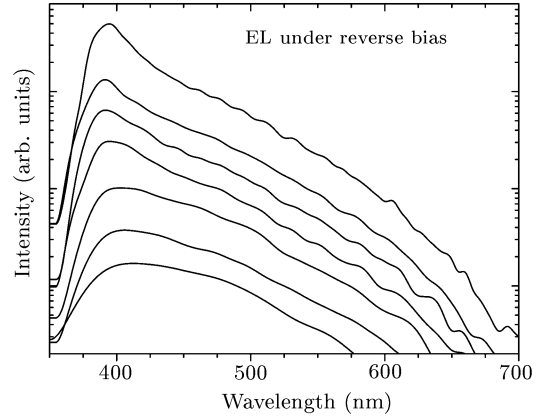


Fig. 2. EL spectra of the *n*-ZnO/*p*-GaN heterojunction under different reverse biases (from 30 V to 90 V in steps of 10 V, with the sequence from bottom to top).

To further understand the origin of the EL spectra, we carry out the room-temperature PL measurement of the *p*-GaN/sapphire and *n*-ZnO/*p*-GaN/sapphire samples. Because the penetration depth of the laser is less than 1 μ m, the *n*-ZnO layer dominates the PL of the *n*-ZnO/*p*-GaN/sapphire sample. The PL of the *p*-GaN/sapphire [Fig. 3(d)] shows two high intense ultraviolet emission peaks at 367 nm and 386 nm, as well as a broad yellow band (\sim 570 nm).^[16–18,27,28] The emission at 367 nm corresponds to the band-edge emission of GaN. The peak at 386 nm (3.21 eV) is typical in Mg doped GaN, which comes from the transmission from conduction band to a shallow Mg acceptor.^[21–26] In contrast, for the *n*-ZnO/*p*-GaN/sapphire sample [Fig. 3(c)], we observe a dominant emission at 378 nm corresponding to the band-edge emission of ZnO and a very broad band centred at \sim 650 nm, which is related to the deep level in ZnO.^[29]

The comparison between EL and PL spectra in Fig. 3 strongly suggests that the EL emission of the *n*-ZnO/*p*-GaN heterostructure at forward bias comes from the *p*-GaN, with the emissions at 390 nm and at 570 nm corresponding to the emission related to the transmission from conduction band to a shallow Mg acceptor at 386 nm and the well-known yellow band of GaN, respectively. The red shift of the emission related to a shallow Mg acceptor in EL is perhaps a result of the increased temperature of the device when applied voltage. Due to the large size of the device, its temperature will increase distinctly with the applied voltage. In fact, the donor concentration in *n*-type ZnO is much higher than the acceptor concentration in *p*-type GaN, and most of the depletion region should be located in the *p*-GaN side. In addition, the migration length of electrons is larger than that

of holes. All these consistently support the scenario that electrons inject from the n-ZnO to p-GaN and radiative recombination takes place in p-GaN. As seen from Fig. 3(a), there is no obvious 367 nm emission in the EL spectrum. This can possibly be explained as self-absorption effects in the ZnO layer because wavelength 367 nm is shorter than 378 nm.

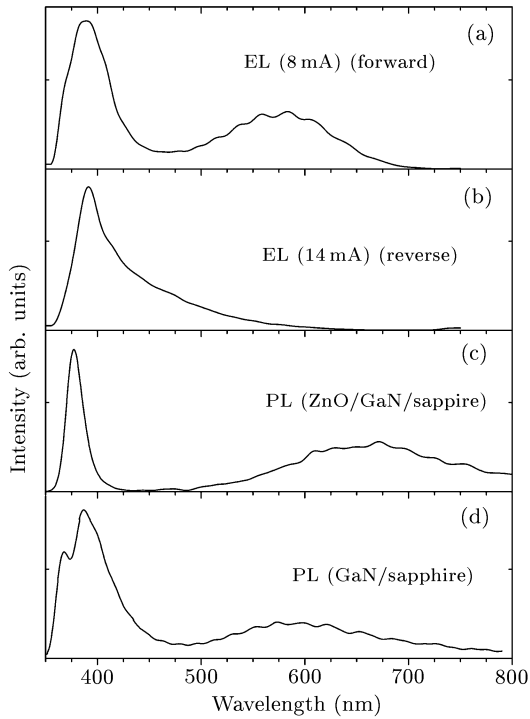


Fig. 3. Comparison of EL with PL of the n-ZnO/p-GaN heterojunction. (a) and (b) EL under forward and reverse biases, (c) PL measured at room temperature using a He-Cd laser, (d) PL from the p-GaN/sapphire sample.

The EL under reverse bias shows only one broad emission at 390 nm and the yellow band is missing. Considering its appearance under both forward and reverse biases and the exponentially reverse-bias dependence, we conclude that the 390 nm emission corresponds to the radiative recombination in the depletion region of p-GaN. Obviously, the light emission behaviour under reverse bias are different from that of conventional forward biased LED. To find the origin, two possible reasons tunnelling and avalanche processes related emission are considered. There is no long tail at the high energy part of the EL spectrum and there is no localized light-emitting spots observed, which are typical in the luminescence during avalanche breakdown,^[30–32] so the avalanche assisted emission is excluded. Therefore, the tunnelling assisted carrier transport could be a possible reason to explain the emission in the p-GaN/n-ZnO heterojunction under a reverse bias similar to the previous report.^[14] As shown in the inset of Fig. 4(b), the n-ZnO/p-GaN heterostructure exhibits a type-II band alignment. The

valence band offset is calculated to vary from 1.0 eV to 2.2 eV and the average value is 1.6 eV depending on the interface configuration.^[33] According to our experimental result of a thin tunnelling barrier, the band offset should be in a high level between 1.6 eV to 2.2 eV. Under a small reverse bias, the occupied valence band of p-GaN will be aligned with or higher than the unoccupied conduction band of n-ZnO, and tunnelling of carriers will occur.

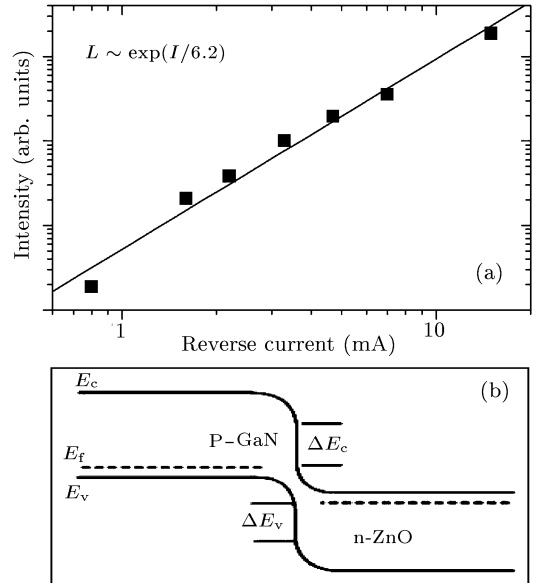


Fig. 4. (a) Luminescence intensity change as a function of the injected current ($L-I$) of the n-ZnO/p-GaN heterojunction under reverse bias. (b) A schematic energy band diagram of the n-ZnO/p-GaN heterojunction under a low reverse voltage.

To further understand the emission of the n-ZnO/p-GaN heterostructure under reverse bias, the light intensity-current ($L-I$) relation is illustrated in Fig. 4(a). An exponential dependence ($L \sim \exp(I/6.2)$) is clearly evidenced at a weak light emission scale. It is shown that more electrons take part in the process of radiative recombination with larger reverse current. In addition, the defects in the materials are probably responsible for some part of reverse current.^[13] With reverse bias increasing, the transmission probability increases exponentially, and the electrons joining the process of radiative recombination increase, leading to the exponential dependence of L versus I .

It is more interesting that the broad yellow band is lost under reverse bias. The yellow band has been studied extensively,^[16–19,22,23] and several different models have been proposed. While the recombination between deep donor states and shallow effective-mass acceptor states was suggested to be a cause,^[22,23] more studies support that it is due to radiative recombination from a near-conduction-band-edge state

to a deep localized acceptor state.^[16–19] Our results are obviously consistent with the latter model. Under the reverse bias, the recombination emission occurs in the depletion region of p-GaN, where the holes are depleted and the deep acceptor states are filled by electrons. The lifetime of these deep energy electrons are so long that they contribute little to the tunnelling. In addition, only the 390 nm emission is related to the transmission from the conduction band to a shallow Mg acceptor. If the yellow band also comes from the shallow acceptor, it should also appear in the spectrum. Therefore, recombination from a higher energy state to a deep localized acceptor state becomes more impossible, leading to the disappearance of the yellow band, as observed at present.

In conclusion, n-ZnO films were grown on p-GaN and an n-ZnO/p-GaN heterostructure-based LED was fabricated and characterized by EL and PL. Different EL spectra under forward and reverse biases were observed. We interpret the unusual EL under reverse bias in terms of a radiative recombination process correlated with the tunnelling carrier transport. Our study provides strong evidence that the well-known yellow band luminescence is caused by recombination from a near conduction band edge state to a deep localized acceptor state.

References

- [1] Bagnall D M, Chen Y F, Zhu Z, Yao T, Koyama S, Shen M Y and Goto T 1997 *Appl. Phys. Lett.* **70** 2230
- [2] Xiang W H, Zhang G Z, Sun Y, Wang G and John B K 2003 *Chin. Phys. Lett.* **20** 296
- [3] Liu M J and Kim H K 2004 *Appl. Phys. Lett.* **84** 173
- [4] Liang W Y and Yoffe A D 1969 *Phys. Rev. Lett.* **20** 59
- [5] Look D C 2001 *Mater. Sci. Eng.* **B 80** 383
- [6] Look D C, Reynolds D C, Litton C W, Jones R L, Eason and Cantwell 2002 *Appl. Phys. Lett.* **81** 1830
- [7] Look D C 2002 *Abstract Booklet, Second International Workshop on Zinc Oxide* (Dayton, OH: Wright State University)
- [8] Sukit L, Zhang S B, Wei S H and Park C H 2004 *Phys. Rev. Lett.* **92** 155504
- [9] Lee E C and Chang K J 2004 *Phys. Rev. B* **70** 115210
- [10] Vispute R D, Talyansky V, Choopun S, Sharma R P, Venkatesan T, He M, Tang X, Halpern J B, Spencer M G, Li Y X, Salamanca-Riba L G and Iliadis A A 1998 *Appl. Phys. Lett.* **73** 348
- [11] Hong S K, Hanada T, Makino H, Chen Y f, Ko H J, Yao T, Tanaka A, Sasaki H and Sato S 2001 *Appl. Phys. Lett.* **78** 3349
- [12] Alivov Y I, Kalinin E V, Cherenkov A E, Look D C, Ataev B M, Omaev A K, Chukichev M V and Bagnall D M 2003 *Appl. Phys. Lett.* **83** 4719
- [13] Alivov Y I, Van Nostrand J E, Look D C, Chukichev M V and Ataev B M 2003 *Appl. Phys. Lett.* **83** 2943
- [14] Park W I and Yi G C 2004 *Adv. Mater.* **16** 87
- [15] Yu Q X, Xu B, Wu Q H, Liao Y, Wang G Z, Fang R C, Lee H Y and Lee C T 2003 *Appl. Phys. Lett.* **83** 4713
- [16] Perlin P, Suski T, Teisseyre H, Leszczynski M, Grzegory I, Jun J, Porowski S, Boguslawski P, Bernholc J, Chervin J C, Polian A and Moustakas T D 1995 *Phys. Rev. Lett.* **75** 296
- [17] Shan W, Schmidt T J, Yang X H, Hwang S J, Song J J and Goldenberg B 1995 *Appl. Phys. Lett.* **66** 985
- [18] Kim S, Herman I P, Tuchman J A, Doverspike K, Rowland L B and Gaskill D K 1995 *Appl. Phys. Lett.* **67** 380
- [19] Shalish, Kronik L, Segal G, Rosenwaks Y, Shapira Y, Tisch U and Salzman J 1999 *Phys. Rev. B* **59** 9748
- [20] Zheng X H, Chen H, Yan Z B, Li D S, Yu H B, Huang Q and Zhou J M 2004 *J. Appl. Phys.* **96** 1899
- [21] Viswanath A, Shin E, Lee J I, Yu S, Kim D, Kim B, Choi Y and Hong C H 1998 *J. Appl. Phys.* **83** 2272
- [22] Oh E, Park H and Park Y 1998 *Appl. Phys. Lett.* **72** 70
- [23] Smith M, Chen G D, Lin J Y, Jiang H X, Salvador A, Sverdlov B N, Botchkarev A, Morkoç H and Goldenberg B 1996 *Appl. Phys. Lett.* **68** 1883
- [24] Kaufmann U, Kunzer M, Maier M, Obloh H, Ramakrishnan A, Santic B and Schlotter P 1998 *Appl. Phys. Lett.* **72** 1326
- [25] Götz W, Johnson N M, Walker J, Bour D P and Street R A 1996 *Appl. Phys. Lett.* **68** 667
- [26] Reshchikov M A, Yi G C and Wessels B W 1999 *Phys. Rev. B* **59** 13176
- [27] Glaser E R, Kennedy T A, Crookham H C, Freitas J A, Asif Khan M Jr, Olson D T and Kuznia J N 1993 *Appl. Phys. Lett.* **63** 2673
- [28] Glaser E R, Kennedy T A, Doverspike K, Rowland L B, Gaskill D K, Freitas J A, Asif Khan M Jr, Olson D T, Kuznia J N and Wickenden D K 1995 *Phys. Rev. B* **51** 13326
- [29] Studenikin S A, Golego N and Cocivera M 1998 *J. Appl. Phys.* **84** 2287
- [30] Chynoweth A G and McKay K G 1956 *Phys. Rev.* **102** 369
- [31] Chynoweth A G and Pearson G L 1958 *J. Appl. Phys.* **29** 1103
- [32] Pilkuhn M and Rupperecht H 1965 *J. Appl. Phys.* **36** 684
- [33] Nakayama T and Murayama M 2000 *J. Cryst. Growth* **214** 299